Available online at www.sciencedirect.com

SCIENCE DIRECT®

Biochimica et Biophysica Acta 1637 (2003) 135–141

BIOCHIMICA ET BIOPHYSICA ACTA

BBA

www.bba-direct.com

Anti-apoptotic proteins are oxidized by $A\beta_{25-35}$ in Alzheimer's fibroblasts

Joungil Choi[a], Christina A. Malakowsky[a], John M. Talent[a], Craig C. Conrad[a], Christopher A. Carroll[b], Susan T. Weintraub[b], Robert W. Gracy[a,*]

[a] *Molecular Aging Unit, Department of Molecular Biology and Immunology, University of North Texas Health Science Center, 3500 Camp Bowie Blvd., Fort Worth, TX 76107, USA*

[b] *Department of Biochemistry, University of Texas Health Science Center at San Antonio, San Antonio, TX 78229, USA*

Received 7 November 2002; accepted 12 December 2002

Abstract

We have examined the effects of the beta-amyloid peptide ($A\beta_{25-35}$) on fibroblasts derived from subjects with Alzheimer's disease (AD) and from age-matched controls. The peptide was significantly more cytotoxic to the AD-derived fibroblasts. The level of protein oxidation was also greater in the cells from AD subjects. Two-dimensional electrophoresis (2-DE) coupled with immunostaining for protein carbonylation revealed specific oxidation-sensitive proteins (OSPs) in both the control and AD-derived cells. Two specific OSPs were identified by mass spectrometry as heat shock protein 60 (HSP 60) and vimentin. Exposure of the cells to $A\beta_{25-35}$ resulted in a twofold increase in the level of oxidation of these two OSPs in the cells derived from controls, but a ninefold increase in their level of oxidation in the fibroblasts from AD subjects. These observations are of particular interest because of the proposed anti-apoptotic roles of both HSP 60 and vimentin and our recent observation that these same two proteins are particularly susceptible to oxidation in neuronally derived cells.

Keywords: Protein oxidation; Two-dimensional gel electrophoresis; Heat shock protein 60; Vimentin; Anti-apoptotic protein; Alzheimer's disease

1. Introduction

The neuropathological hallmarks of Alzheimer's disease (AD) are accumulation of extracellular amyloid senile plaques and intracellular neurofibrillary tangles. The main constituent of senile plaques is beta-amyloid (Aβ), which is believed to induce or exacerbate oxidative stress that is central to the pathology [1–4]. Studies have shown an elevated oxidative modification of proteins, lipids, and DNA in the brain of AD subjects [5,6]. Aβ has been shown to cause both neuronal membrane peroxidation and protein oxidation, and its cytotoxicity is prevented by antioxidants [7,8]. Although the neurotoxic activity of Aβ is thought to be mediated by hydrogen peroxide and perhaps other reactive oxygen species (ROS) [9,10], the cellular targets of Aβ-mediated oxidations remain unclear.

Side chains of virtually all types of amino acids in proteins can be oxidized, but the susceptibility of protein to oxidative modification is highly dependent on its sequence and overall structure [1]. Oxidation can alter protein functions in many ways (e.g. directly modifying catalytic amino acids, critical residues in binding sites, or regulatory sites; and by changing proteolytic susceptibility, states of aggregation, etc.). Therefore, identification of specific oxidation-sensitive proteins (OSPs) may provide important clues to understanding of the role of oxidative damage in the pathology of the disease.

Although AD is generally considered a neurological disorder, numerous changes in tissues other than brain of AD patients have been reported, suggesting that it is systemic. For example, peripheral abnormalities include mitochondrial uncoupling, deficiencies in several key enzymes, altered oxidative metabolism, abnormal amyloid precursor protein metabolism, and altered calcium homeostasis in platelets and other blood cells [11–13]. Thus,

Abbreviations: DNPH, 2,4-dinitrophenylhydrazine; PVDF, polyvinylidene difluoride; DNP-antibody, dinitrophenyl-antibody; PBS, phosphate buffered saline; SDS, sodium dodecyl sulfate; ROS, reactive oxygen species; 2-DE, two-dimensional electrophoresis; IPG, immobilized pH gradient; HSP 60, heat shock protein 60; DCFH-DA, 2′, 7′-dichlorofluorescin diacetate; MALDI-TOF/MS, matrix-assisted laser desorption ionization time-of-flight mass spectrometry; ESI-MS^n, electrospray tandem mass spectrometry; 2D-PAGE, two-dimensional polyacrylamide gel electrophoresis

* Corresponding author. Tel.: +1-817-735-5400; fax: +1-817-735-5485.

E-mail address: rgracy@hsc.unt.edu (R.W. Gracy).

0925-4439/03/$ - see front matter © 2003 Elsevier Science B.V. All rights reserved.
doi:10.1016/S0925-4439(02)00227-2

fibroblasts from Alzheimer's subjects may provide a cellular model system in which the effects of amyloid beta protein on protein oxidation can be monitored in the dynamic state and provide information on the mechanism of pathogenesis.

In this study, we investigated the effect of the 11-residue beta-amyloid peptide ($A\beta_{25-35}$) on protein oxidation and cytotoxicity in fibroblasts from AD subjects and age-matched controls. Furthermore, we sought to identify the critical OSPs that are susceptible to oxidative damage in cells from AD subjects. To achieve this, we separated proteins by two-dimensional electrophoresis (2-DE) and immunostained with an anti-DNP antibody to visualize oxidized proteins [14]. The most easily oxidized proteins were identified by mass spectrometry.

2. Materials and methods

2.1. Chemicals

Sodium dodecyl sulfate (SDS), 2,4-dinitrophenylhydrazine (DNPH), urea, acrylamide, HCl, glutaraldehyde, formaldehyde, Tris-base, and other general chemicals suitable for electrophoresis were purchased from Fisher Scientific (Houston, TX) or VWR Scientific Products (Houston, TX).

2.2. Cell culture

Human skin fibroblasts were obtained from the Coriell cell repository (Camden, NJ). These cells were cultured as described previously [15] using standard Dulbecco's modified eagle medium (DMEM) with 10% (w/v) fetal bovine sera and gentomycin. Cells were maintained in T-75 flasks until they were confluent.

2.3. Beta-amyloid ($A\beta_{25-35}$) treatment

$A\beta_{25-35}$ peptide was dissolved in sterile water to a concentration of 1 mg/ml and diluted with media to the desired concentrations. It should be noted that the smaller cytotoxic $A\beta_{25-35}$ peptide was used rather that the full $A\beta_{1-42}$ and at higher concentrations than exist in vivo. The specificity of the toxicity of the peptide was confirmed since use of the reverse sequence ($A\beta_{35-25}$) was nontoxic under these conditions. For cell viability studies, the day before an experiment, cells were plated in 96-well plates at a density of 4×10^3 cells per well. For protein separation by two-dimensional polyacrylamide gel electrophoresis (2D-PAGE), cells were plated in 100-mm culture dishes at a density of 2×10^6 cells per plate. The cells were treated with $A\beta_{25-35}$ at a final concentration of 94 μM.

2.4. Cell viability

Cell viability was measured using a formazan assay kit (Promega, Madison, WI) [16]. The conversion of MTS into the aqueous soluble formazan by the dehydrogenases in metabolically active cells was quantified from the absorbance at 490 nm. In order to correct for growth that occurred during experiments, absorbance values for treated cells were divided by the respective absorbance values for nontreated cells.

2.5. Measurement of ROS generated by $A\beta_{25-35}$

ROS generated intracellularly were assessed using the probe 2′, 7′-dichlorofluorescin diacetate (DCFH-DA) (Molecular Probes Inc., Eugene, OR). DCFH-DA is freely permeable and enters the cell where cellular esterases hydrolyze the acetate moieties, trapping the polar DCFH in the cell. ROS in the cells oxidize the DCFH, yielding the fluorescent product 2′, 7′-dichlorofluorescin (DCF) [17]. Cells were seeded into 96-well plates as described above. On the third day of the incubation with $A\beta_{25-35}$, DCFH-DA loading-medium was added (containing DCFH-DA at 50 μM). The cells were incubated in 5% CO_2/95% air at 37 °C for 45 min. After removing the excess DCFH-DA, cells were washed twice with phosphate buffered saline (PBS) and incubated in phenol red-free DMEM medium containing 10% (v/v) FBS. The fluorescence of the cells was measured with a Bio-Tek microplate fluorescence reader FL-600 with excitation at 485 ± 20 nm and emission at 530 ± 25 nm.

2.6. Sample preparation

Approximately 2×10^6 cells were plated in 100-mm plates, allowed to attach for 12 h, and then exposed to the different experimental conditions. Cells were then trypsinized, collected via centrifugation ($1000 \times g$, 10 min), washed three times in PBS, and recollected by centrifugation. The cellular pellet was then dissolved in dSDS buffer [0.3% (w/v) SDS; 1% (w/v) BME; 0.05 M Tris–HCl, pH 8.0] and passed through a 22-gauge needle 10 times. The extract was placed in boiling water for 3 min and then transferred to ice for 10 min. Protease inhibitor cocktail (Complete™, Fisher), DNase (M610A: Promega), and RNase (732-6349: Bio-Rad, Hercules, CA) were added, and the solution placed at 37 °C for 1 h. Particulates were removed by centrifugation ($15{,}000 \times g$, 15 min), and the supernatant solution was collected. Because the dSDS solution interferes with protein quantification, proteins in a 20-μl aliquot were precipitated with TCA and the precipitate reconstituted in BCA protein reagent [18] (Pierce, Rockford, IL).

2.7. Isoelectric focusing and 2D-PAGE

Protein samples (250 μg) were absorbed onto 18-cm immobilized pH gradient (IPG) strips (pH 5–6) in an IPG re-swelling tray, and the strips then isoelectrically focused on a Multiphor II (Amersham Biosciences, Piscataway, NJ)

Table 1
Cytotoxicity of $A\beta_{25-35}$ to fibroblasts from Alzheimer's subjects

Cell line ID#	Diagnosis	Donor age	Percent cell survival in the presence of $A\beta_{25-35}$			
			Incubation time			
			24 h	48 h	72 h	96 h*
AG 14048	Control	71	108 ± 20	104 ± 8	89 ± 7.9	77 ± 8.9
AG 13245	Control	68	99 ± 15.7	100 ± 12.4	86 ± 11.4	75 ± 6.4
AG 13983	Control	71	98 ± 17.3	100 ± 14	92 ± 6.6	83 ± 13.1
AG 07374	AD (clinically)	73	105 ± 14.4	102 ± 15.7	81 ± 9.9	54 ± 5.1
AG 08243	AD (clinically)	72	96 ± 12	106 ± 9	85 ± 8.1	46 ± 7.3
AG 08527	AD (autopsy confirmed)	61	99 ± 8	98 ± 11	82 ± 10.1	47 ± 9.6

The percent cell survival for each time point was corrected for the growth of the cells by dividing the absorbance value of the treated cells ($A\beta_{25-35}$) by the absorbance value of the corresponding nontreated cells. The value of percent cell survival is the mean of seven samples.

*Cell death of the fibroblasts from AD increased significantly ($p < 0.001$ by ANOVA) compared to control fibroblasts at 96-hour time point.

for 24,000 V/h [19]. Following isoelectric focusing the strips were immediately DNP-derivatized (as described below), then subjected to equilibration for 15 min in 50 mM Tris–HCl (pH 8.8) containing 6 M urea, 2% (w/v) SDS, 30% (v/v) glycerol, and 1.0% (w/v) dithiothreitol. Strips were then re-equilibrated for 15 min in the same buffer containing 2.5% (w/v) iodoacetamide in place of dithiothreitol. In all cases, molecular weight separation was achieved using the ISO-DALT slab gel SDS-PAGE system (Amersham Biosciences).

2.8. Derivatization of protein carbonyls

Protein samples were derivatized by the "in-strip DNP derivatization method" of Conrad et al. [14]. Following rehydration and isoelectric focusing, the IPG strips were placed in 25-ml test tubes and incubated for 15 min in 2 N HCl/10 mM DNPH at 25°C. After the reaction, the strips were washed once with 2 M Tris-base/30% (v/v) glycerol for 15 min. Sample IPG strips were then prepared for molecular weight separation as described above.

2.9. Sypro® Ruby protein gel stain staining

Duplicate samples of the derivatized proteins were separated on SDS gradient-polyacrylamide gels (e.g. 9–15% porosity polyacrylamide). Proteins in one gel were stained with Sypro® Ruby protein gel stain (Bio-Rad), while proteins on the duplicate gel were electroblotted to polyvinylidene difluoride (PVDF) membranes using the ISO-DALT system. Proteins were first fixed in the gel using 40% methanol/10% acetic acid (v/v) for 30 min. The protein gel was then incubated in Sypro® Ruby protein gel stain solution overnight and subsequently destained using 10% methanol/ 6% acetic acid (v/v) for 45 min. The gels were placed in a light-tight cabinet directly on a transilluminator; the dye was then excited with UV light at 365 nm and a cooled, computerized CCD camera-based imaging system (Alpha Innotech Corporation, San Leandro, CA) was used to record the fluorescence.

2.10. DNP-immunostaining

The PVDF membranes were removed from the ISO-DALT electroblotting apparatus and incubated for 1 h with 5% (w/v) skim milk powder dissolved in PBS containing 3% (v/v) Tween (PBS–Tween). Membranes were incubated overnight at 4 °C with the anti-DNP primary antibody (Molecular Probes) solution [1:16,000 dilution in PBS–Tween containing 5% (w/v) milk] as described previously [20]. The membranes were then washed three times (15 min each) with PBS–Tween, incubated for 1 h at 4 °C with a 1:16,000 dilution of the goat anti-rabbit [horse radish peroxidase (HRP) conjugated] secondary antibody (Sigma, St. Louis, MO) in PBS–Tween containing 5% (w/v) milk, and subsequently washed three times (15 min each) with PBS–Tween. A chemiluminescence kit (SuperSignal West Femto Maximum Sensitivity Substrate; Pierce) and a cooled, computerized CCD camera-based imaging system (Alpha Innotech) were used to visualize and record the stained proteins.

2.11. Protein image analysis and 2-DE database

The digitized images from the gels stained with Sypro® Ruby for total protein, and from the immunostained blots, were analyzed using the 2-DE gel analysis program Melanie 3 (Geneva Bioinformatics, Geneva, Switzerland). A comparison report of qualitative and quantitative differences of specific proteins on each gel set of data was then generated.

Table 2
Reactive oxygen species generation

Fibroblasts	2,7-DCF fluorescence/MTS
Non-AD control	1.26 ± 0.05
AD	1.24 ± 0.037

Fibroblasts were incubated in 94 μM $A\beta_{25-35}$ for 3 days. Levels of cellular oxidative stress generated by beta-amyloid were measured relative to control cells incubated in the absence of $A\beta_{25-35}$. ROS were measured from fluorescence of DCF as described in Materials and methods and are expressed as relative fluorescence intensity per level of cell viability as measured by the MTS assay. Values are means ± S.E. of nine samples.

2.12. Mass spectrometry analysis

Spots of interest were excised from the gel and digested in situ with trypsin (modified; Promega). The resulting digests were analyzed by mass spectrometry (MALDI-TOF/MS using an Applied Biosystems Voyager DE-STR and capillary-HPLC-ESI/MS/MS on a Thermo Finnigan LCQ). The peptide mass maps produced by MALDI-TOF/MS were

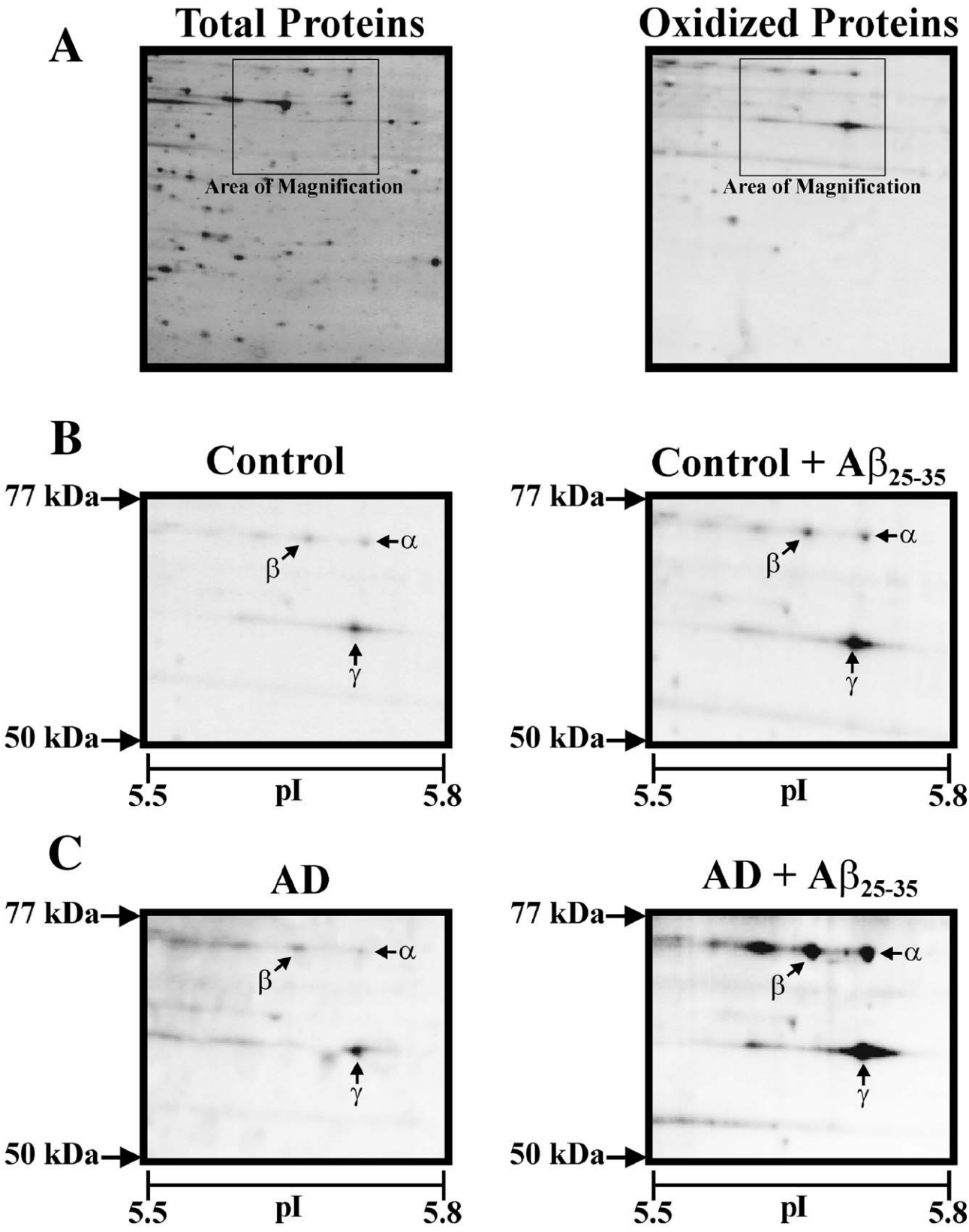

Table 3

Fig. 1, panels B and C	Treatment	Specific oxidation index[a]		
		α	β	γ
Control fibroblast	none	60 ± 2	63 ± 26	214 ± 56
Control fibroblast	94 μM β-amyloid	132 ± 24	118 ± 30	472 ± 88
AD fibroblast	none	55 ± 20	62 ± 18	246 ± 71
AD fibroblast	94 μM β-amyloid	559 ± 87	593 ± 94	1113 ± 215

[a] Specific oxidation index (e.g. nanomoles of carbonyl per milligram of protein) [26].

searched against the published databases by means of the MS-Fit module in Protein Prospector http://prospector.ucsf.edu/ucsfhtml3.4/msfit.htm) and Mascot (Matrix Science, http://www.matrixscience.com). The uninterpreted HPLC-ESI/MS/MS data were analyzed by SEQUEST, a component of the LCQ software and by Mascot.

3. Results

Table 1 shows the cell survival of human fibroblasts from AD patients and age-matched controls. $A\beta_{25-35}$ was not noticeably toxic to either the human fibroblasts from AD or age-matched controls until more than 2 days had elapsed. Both types of cells began to experience cytotoxicity after a 3-day incubation with $A\beta_{25-35}$, and the viability of the AD-derived fibroblasts was significantly lower than controls ($P<0.001$ by ANOVA). Concurrent with cell survival assays, the cells were visualized at 10× magnification by light microscopy. Throughout the 4 days, untreated control cells exhibited typical elongated, flat fibroblast morphology. However, at day 3 and thereafter, some of the treated AD cells began to exhibit morphological changes (e.g. became spherical). Over half of the cells were dead after a 4-day incubation with beta-amyloid.

The levels of ROS generated by $A\beta_{25-35}$ were similar in fibroblasts from both AD and age-matched controls (Table 2). This indicates that fibroblasts from AD and controls do not differ in their ability to take up the DCFH. The different susceptibility of these cells to the oxidative stress does not appear to be due to different levels of production of ROS by $A\beta_{25-35}$.

In pilot studies, one-dimensional gel electrophoresis was used to evaluate the level of oxidation of proteins after incubating cells in the presence and absence of $A\beta_{25-35}$. While the AD cells exhibited slightly greater levels of oxidized proteins after 1 and 2 days, by day 3 the level of oxidation of proteins in the fibroblasts from the AD subjects was approximately threefold greater than from the controls (data not shown).

Table 4
Protein identification using MALDI-TOF/MS

Spot name	Protein MW (Da)/p*I*	Identification (accession number)
α	61055/5.7	Heat shock protein 60 (284763)
β	61055/5.7	Heat shock protein 60 (284763)
γ	53686/5.1	Vimentin (P08670)

Summary of the protein properties (theoretical isoelectric point and molecular weight) and identification of proteins using MALDI-TOF.

In order to determine which specific proteins were oxidized, we utilized 2-DE. Fig. 1A (left panel) shows a typical example of a human skin fibroblast extract separated by 2-DE (18-cm IPG strip: pH 5–6) and Sypro® Ruby-stained for total proteins. Fig. 1A (right panel) shows the immunostained protein profile on the Western blot after probing with anti-DNP antibody to detect the oxidized proteins. Fig. 1B and C represents the immunostained protein profiles from the area of magnification in Fig 1A, right panel. Only a few of the proteins were oxidized and all were located in the area defined by: p*I* = 5–6, MW = 50–80 kDa. Fibroblasts from both AD and age-matched controls showed basal levels of oxidation of these particular proteins even when there was no exposure to $A\beta_{25-35}$. The level of oxidation of these proteins in the fibroblasts from AD subjects after exposure to $A\beta_{25-35}$ was increased 9- to 10-fold from control levels for "α"and "β", and 4.5-fold for "γ" (Table 3). In contrast, the fibroblasts from age-matched controls under the same conditions showed only an approximate twofold increase in oxidation. This indicates that these specific proteins are susceptible to oxidation in fibroblasts from both AD and age-matched controls. However, the levels of oxidation of all three proteins were much higher in the fibroblasts from AD compared to the non-AD controls. These three OSPs were excised from the gels and identified by mass spectrometry. Two of the proteins ("α" and "β") were identified as isoforms of heat shock protein 60 (HSP 60); the third OSP ("γ") was identified as vimentin (Table 4).

4. Discussion

Elevated levels of beta-amyloid protein and its deposition within the senile plaques of the brain are a hallmark of the pathology of AD. Beta-amyloid has been shown to produce ROS, which are believed to cause the accumulation of oxidatively damaged proteins, which ultimately lead to neuronal apoptosis [8,9]. Furthermore, the lesions in the AD brain reveal oxidative damage by free radicals [5,6]. Beta-amyloid can exist in either soluble or fibril forms. The

Fig. 1. Effect of $A\beta_{25-35}$ treatment on specific protein oxidation. Exponentially dividing cells were dissociated with trypsin, and approximately 1×10^6 cells were plated into 100-mm plates and allowed to attach. Following a 3-day exposure of cells to 94 μM $A\beta_{25-35}$, both treated and nontreated cell extracts were collected, then subjected to isoelectric focusing (18-cm IPG strips, pH 5–6) and molecular weight separation, as described in Materials and methods. Panel A shows a 2-DE gel of a treated AD fibroblast sample that was Sypro® Ruby-stained in order to visualize all proteins, and a blot immunostained with antibody against DNP to visualize oxidized proteins having new DNP-reactive carbonyl groups. Panels B and C represent enlarged views of the area that shows the highest intensity immunostaining: three specific oxidized proteins are highlighted (α, β, and γ).

aggregated fibril form, which is self-generated from several days of incubation of soluble form, exhibits greater cytotoxicity and increased production of ROS [21]. In our studies, cells were not noticeably affected until after 2 days of incubation with beta-amyloid. These results were observed in the cell survival assay, in light microscopy, and in analysis of levels of oxidized proteins. The measurement of ROS produced inside cells showed a negligible difference between nontreated and beta-amyloid treated samples through the first 2 days of incubation with beta-amyloid. However, after the third day of beta-amyloid incubation, the levels of DCF-fluorescence were increased in the beta-amyloid-treated cells compared to the nontreated cells. This lag time may be due to the time required for the formation of aggregated beta-amyloid (approximately 3 days) [22]. The levels of DCF-fluorescence, however, were similar in fibroblasts from both AD and controls, indicating no difference in ability to produce ROS inside cells by $A\beta_{25-35}$. The different susceptibility (shown by cell survival, cell morphology, and protein oxidation) of $A\beta_{25-35}$-treated fibroblasts from AD subjects, compared to age-matched controls, suggests inherent differences in the AD fibroblasts (e. g. diminished antioxidant capacity).

The most readily oxidized proteins (designated "α", "β", and "γ") identified by mass spectrometry were HSP 60 ("α" and "β") and vimentin ("γ"). The two isoforms of HSP 60 appear to differ only in charge (isoelectric point), and thus are most likely produced by different degrees of oxidation. HSP 60 plays a role as a mitochondrial chaperon and its overexpression protects cells from apoptosis [23]. Vimentin is a critical cytoskeleton protein that is cleaved by caspases at an early stage of apoptosis [24]. The overexpression of caspase-resistant vimentin protects the cells from apoptotic cell death caused by oxidative stresses in vitro [25]. Thus, the two proteins, which appear to be most easily oxidized in the human skin fibroblasts from AD patients, are both antiapoptotic proteins. We also recently observed that these two proteins appeared to be the primary targets of H_2O_2-induced oxidative stress in neuronal cells [26]. The oxidation of both HSP 60 and vimentin by either H_2O_2 or $A\beta_{25-35}$ suggests that H_2O_2 may be the mediator of the $A\beta_{25-35}$ toxicity. This would be consistent with previous reports of H_2O_2 production by beta-amyloid [27].

The involvement of oxidation in the induction of the apoptosis is well established in both cell culture and animal models [28,29]. By damaging specific proteins, such as redox-sensitive regulatory proteins or apoptosis-related proteins, oxidative stress can cause direct cell injury and alter the cellular signaling system. For example, the transcription factor NF-κB is bound to the inhibitory protein IκB in the cytoplasm. When cells are exposed to oxidative stress, IκB becomes oxidized and loses its inhibitory function, resulting in the activation of NF-κB [30–37]. The identification of such OSPs is critical for understanding the relationship between oxidative stress and cell death, and perhaps the underlying etiology of AD. Clearly, additional studies on these particular OSPs and the reasons they are more susceptible to oxidation in AD-derived cells are of major interest.

Acknowledgements

The authors acknowledge the support of the Institutional Mass Spectrometry Laboratory at the University of Texas Health Science Center at San Antonio (supported in part by NIH grant CA54174) for mass spectrometric analyses. This research was supported by grants from the Alzheimer's Association (IIRG-98-037), the Interdependent Alzheimer's Disease Core Facilities sponsored by an Alzheimer's Intramural Research Grant, and the Texas ATP/ARP program (#000130-0025-2001).

References

[1] B.S. Berlett, E.R. Stadtman, J. Biol. Chem. 272 (1997) 20313–20316.
[2] K. Hensley, N. Hall, R. Subramanian, P. Cole, D.A. Butterfield, J. Neurochem. 65 (1995) 2146–2156.
[3] L.J. McIntosh, M.A. Trush, J.C. Troncoso, Free Radic. Biol. Med. 23 (1997) 183–190.
[4] W.R. Markesbery, J.M. Carney, Brain Pathol. 9 (1999) 133–146.
[5] M.J. Foster, A. Dubey, K.M. Dawson, W.A. Stutts, H. Lal, R.S. Sohal, Proc. Natl. Acad. Sci. U. S. A. 93 (1996) 4765–4769.
[6] C.D. Smith, J.M. Carney, P.E. Starke-Reed, C.N. Oliver, E.R. Stadtman, R.A. Floyd, Proc. Natl. Acad. Sci. U. S. A. 88 (1991) 540–543.
[7] C. Behl, J. Davis, G.M. Cole, D. Schubert, Biochem. Biophys. Res. Commun. 186 (1992) 944–950.
[8] D.A. Butterfield, Chem. Res. Toxicol. 10 (1997) 495–506.
[9] C. Behl, J.B. Davis, R. Lesley, D. Schubert, Cell 77 (1994) 1–20.
[10] M.E. Harris, K. Hensley, D.A. Butterfield, R.A. Leedle, J.M. Carney, Exp. Neurol. 131 (1995) 193–202.
[11] J.P. Blass, A.C. Baker, L. Ko, R.S. Black, Arch. Neurol. 47 (1990) 864–869.
[12] G. Gibson, P. Nielsen, V. Mykytyn, K. Carlson, J. Blass, Neurochem. Res. 14 (1989) 17–24.
[13] S. Govoni, L. Gasparini, M. Racchi, M. Trabucchi, Life Sci. 59 (1996) 461–468.
[14] C.C. Conrad, P.L. Marshall, J.M. Talent, C.A. Malakowsky, R.W. Gracy, Biochem. Biophys. Res. Commun. 275 (2000) 678–681.
[15] R.W. Gracy, K.Ü. Yüksel, T.M. Jacobson, M.L. Chapman, J.C. Hevelone, G.E. Wise, S.D. Dimitrijevich, in: H.P. von Hahn, J. Andrews, M. Ermini (Eds.), Gerontology: Cellular Models and Tissue Equivalent Systems for Evaluating the Structures and Significance of Age-Modified Proteins, vol. 37, S. Karger AG, Basel, Switzerland, 1991, pp. 113–127.
[16] A.H. Cory, T.C. Owen, J.A. Barltrop, J.G. Cory, Cancer Commun. 3 (1991) 207–212.
[17] Z.X. Yao, K. Drieu, V. Papadopoulous, Brain Res. 889 (2001) 181–190.
[18] A.J. Link, Methods Mol. Biol. 112 (1999) 49–52.
[19] J.M. Talent, Y. Kong, R.W. Gracy, Anal. Biochem. 263 (1998) 31–38.
[20] C.C. Conrad, J.M. Talent, C.A. Malakowsky, R.W. Gracy, Biol. Proced. Online 2 (2000) 39–45.
[21] C.J. Pike, D. Burdick, A.J. Walencewicz, C.C. Glabe, C.W. Cotman, J. Neurosci. 13 (1993) 1676–1687.
[22] A. Lorenzo, B.A. Yankner, Proc. Natl. Acad. Sci. U. S. A. 91 (1991) 12243–12247.

[23] M.L. Kurt, L. Brian, Y.L. Ian, M. Ruben, E.S. Immo, H.D. Wolfgang, Circulation 103 (2001) 1787–1792.
[24] Y. Byun, F. Chen, R. Chang, M. Trivedi, K.J. Green, V.L. Cryns, Cell Death Differ. 8 (2001) 443–450.
[25] I. Belichenko, N. Morishima, D. Separovic, Arch. Biochem. Biophys. 390 (2001) 57–63.
[26] J. Choi, C. Conrad, R. Dai, C. Malakowsky, et al., Proteomics, (in press).
[27] X. Huang, C.S. Atwood, M.A. Hartshorn, G. Multhaup, L.E. Goldstein, R.C. Scarpa, M.P. Cuajungco, D.N. Gray, J. Lim, R.D. Moir, R.E. Tanzi, A.I. Bush, Biochemistry 38 (1999) 7609–7616.
[28] R. Etcheberrigaray, J.L. Payne, D.L. Alkon, Life Sci. 59 (1996) 491–498.
[29] F.J. Ekinci, M.D. Linsley, T.B. Shea, Brain Res. Mol. Brain Res. 76 (2000) 389–395.
[30] A.A. Beg, A.S. Baldwin Jr., Genes Dev. 7 (1993) 2064–2070.
[31] A.A. Beg, D. Baltimore, Science 274 (1996) 782–784.
[32] S. Ghosh, et al., Cell 62 (1990) 1019–1029.
[33] M. Kieran, V. Blank, F. Logeat, J. Vandekerckhove, et al., Cell 62 (1990) 1007–1018.
[34] G.P. Nolan, S. Ghosh, H.C. Liou, P. Tempst, D. Baltimore, Cell 64 (1991) 961–969.
[35] S.M. Ruben, et al., [published erratum appears in Science 1991 Oct 4; 254(5028):11]. Science 251 (1991) 1490–1493.
[36] S.C. Sun, P.A. Ganchi, D.W. Ballard, W.C. Greene, Science 259 (1993) 1912–1915.
[37] U. Zabel, T. Henkel, M.S. Silva, P.A. Baeuerle, EMBO J. 12 (1993) 201–211.